scientific reports

Check for updates

OPEN

A bulk form Cu-based ferromagnetic semiconductor (La,Ba)(Cu,Mn)SO with the Curie temperature up to 170 K

Jinou Dong[1], Cui Ding[1], Xueqin Zhao[1], Lingfeng Xie[1], Qiaolin Yang[1], Xun Pan[1], Guoxiang Zhi[1], Licheng Fu[1], Yilun Gu[1] & Fanlong Ning[1,2,3,4]✉

We report the ferromagnetism in a new bulk form Cu-based magnetic semiconductor (La,Ba)(Cu,Mn)SO, which is iso-structural to the prototypical iron-based 1111-type superconductor LaFeAsO. Starting from the parent compound LaCuSO, carriers are introduced via the substitutions of La for Ba while spins are introduced via the substitutions of Cu for Mn. Spins are mediated by carriers, which develops into the long range ferromagnetic ordering. The maximum Curie temperature T_C reaches up to ~170 K with the doping levels of 10% Ba and 5% Mn. By comparing to the (La,Sr)(Cu,Mn)SO where Sr and Mn are co-doped into LaCuSO, we demonstrate that negative chemical pressure would suppress the ferromagnetic ordering.

The discovery of ferromagnetism in III-V semiconductors doped with magnetic atom doping has opened a new window in the research of spintronics[1–5]. It has been proposed that the Curie temperature T_C of (Ga,Mn)As would be raised to room temperature when spin and carrier densities are optimized[6]. Unfortunately, due to the mismatch of valence between Mn^{2+} and Ga^{3+}, the solid solubility is severely limited, hindering more Mn atoms doped in (Ga,Mn)As. As of today, T_C in (Ga,Mn)As has a maximum value of ~ 200 K with Mn doping level up to ~ 12%[7–10]. On the other hand, the non-equivalent substitutions of Mn for Ga in (Ga,Mn)As introduce magnetic moments and carriers simultaneously, which makes it difficult to separate spins and charges, and investigate their individual contributions to the formation of ferromagnetism. Besides, (Ga,Mn)As is fabricated in the form of thin-film by molecular beam epitaxy (MBE) that is extremely sensitive to the preparation process, which makes some research inconclusive[11–13]. Hence, to understand the general mechanism of ferromagnetic ordering and seek for magnetic semiconductors (MSs) with T_C close to room temperature are still the forefront research in spintronics.

Recently, many novel bulk MSs that are the structural derivatives of iron-based superconductors have emerged, such as 111-type Li(Zn,Mn)As (T_C = 50 K)[14], Li(Zn,Mn)P (T_C = 34 K)[15], Li(Zn,Cr)As (T_C = 218 K)[16], 122-type (Ba,K)(Zn,Mn)$_2$As$_2$ (T_C = 230 K)[17,18], N-type Ba(Zn,Co)$_2$As$_2$ (T_C = 45 K)[19] and 1111-type (La,Ba)(Zn,Mn)AsO (T_C = 40 K)[20], which are iso-structural to the iron-based superconductors 111-type LiFeAs[21], 122-type (Ba,K)Fe$_2$As$_2$[22] and 1111-type LaFeAsO$_{1-\delta}$[23], respectively. In these bulk MSs, it has been demonstrated that the long range ferromagnetic ordering is arising from the doped magnetic atoms, and the mechanism of ferromagnetism is the same as that of (Ga,Mn)As[18,20,24]. Furthermore, these bulk MSs have the advantages of decoupled spin and carrier doping, which enables the concentrations of charges and spins to be tuned separately. Thirdly, the bulk form specimens enable the application of magnetic techniques at microscopic level, such as nuclear magnetic resonance (NMR)[25], muon spin relaxation (μSR) and neutron scattering[26,27].

In order to improve T_C, researchers have examined the influence of physical and chemical pressures on MSs. As expected, the effects of pressure on MSs are quite different. It has been shown that the applied physical pressure, positive chemical pressure and negative chemical pressure all suppress the T_C in (Ba,K)(Zn,Mn)$_2$As$_2$[28,29]. On the other hand, the positive chemical pressure would enhance the Curie temperature T_C by 18% in Ba(Zn,Co)$_2$As$_2$[30] and 30% in (La,Ca)(Zn,Mn)AsO[31]. In addition, the bulk MSs mentioned above are all Zn-based MSs.

[1]Zhejiang Province Key Laboratory of Quantum Technology and Device and School of Physics, Zhejiang University, Hangzhou 310027, China. [2]Collaborative Innovation Center of Advanced Microstructures, Nanjing University, Nanjing 210093, China. [3]State Key Laboratory of Silicon and Advanced Semiconductor Materials, Zhejiang University, Hangzhou 310027, China. [4]Science and Technology Innovation Center, Chifeng High-Tech Industrial Development Zone, Chifeng 025250, China. ✉email: ningfl@zju.edu.cn

Apparently, in order to shed light on the origin of ferromagnetism, we also need to pay more attention to other type MSs, such as Cu-based MSs. In past, a new Cu-based MS[32] has been reported with T_C around 200 K when Sr and Mn were co-doped into the parent compound LaCuSO, which is a wide band gap (3.1 eV) semiconductor[33,34]. It is natural to wonder what would happen if Ba (which has larger ionic radius than Sr^{2+}) and Mn are co-doped into LaCuSO, and how chemical pressure would affect the ferromagnetism in 1111-type Cu-based MSs.

In this paper, we report the successful synthesis of a 1111-type bulk MS (La,Ba)(Cu,Mn)SO. Spins are introduced via the substitutions of Cu for Mn, and carriers are introduced via the substitutions of La for Ba into the parent compound LaCuSO. The resultant maximum T_C is ~ 170 K with Ba and Mn doping up to 10% and 5%, respectively. Basing on the experimental results, we unequivocally demonstrate that carriers play important roles in the formation of the ferromagnetism. Comparing to (La,Sr)(Cu,Mn)SO, the Weiss temperature θ of (La,Ba)(Cu,Mn)SO with the same doping levels is about 37% lower, which is apparently due to the reason that the ionic radius of Ba^{2+} is larger than that of Sr^{2+}, that is, negative chemical pressure suppresses the ferromagnetic ordering in (La,AE)(Cu,Mn)SO (AE=Sr, Ba) MS systems.

Results

X-ray diffraction and transport. We show the crystal structure and x-ray diffraction patterns of the samples in Fig. 1. The Bragg peaks in Fig. 1a can be well indexed by a tetragonal ZrCuSiAs-type structure with *P4/nmm* (No.129) space group, indicating that both parent compound LaCuSO and doped compounds are isostructural to the 1111-type iron-based superconductor LaFeAsO[23,34]. In Fig. 1b, we plot the lattice parameters of the specimens obtained by Rietveld refinement. Comparing with the parent compound LaCuSO, all doping samples have larger lattice parameters. No impurity phase has been observed. We show the Rietveld refinement profile of $(La_{0.975}Ba_{0.025})(Cu_{0.95}Mn_{0.05})SO$ in Fig. 1c by using the GSAS-II package as an example, and the resulting weighted reliability factor R_{wp} is ~ 8.3%, implying a well and reliable refinement[35]. In Fig. 1d, we show the electrical resistivity of the $(La_{0.9}Ba_{0.1})(Cu_{0.9}Mn_{0.1})SO$ down to 70 K (It increases beyond the measurement limitation below ~ 70 K). We can see that the resistivity curve retains its semiconducting behavior. According to

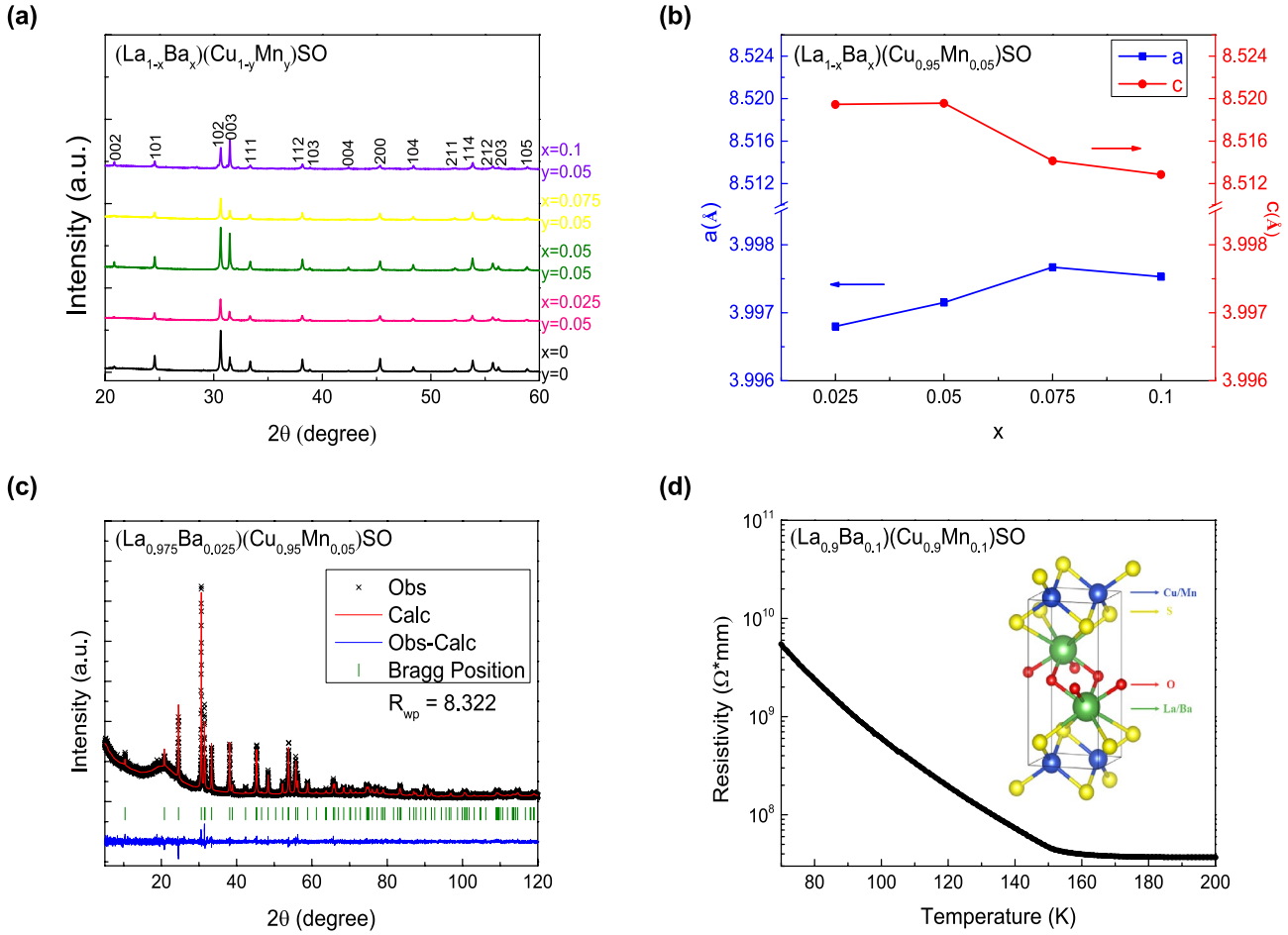

Figure 1. (**a**) The X-ray diffraction patterns for $(La_{1-x}Ba_x)(Cu_{1-y}Mn_y)SO$ ($0 \le x \le 0.1, 0 \le y \le 0.05$) with (hkl) index. (**b**) The lattice parameters *a* and *c* of $(La_{1-x}Ba_x)(Cu_{0.95}Mn_{0.05})SO$ ($0 \le x \le 0.1$). (**c**) The Rietveld refinement of $(La_{0.975}Ba_{0.025})(Cu_{0.95}Mn_{0.05})SO$. (**d**) The electrical resistivity of the $(La_{0.9}Ba_{0.1})(Cu_{0.9}Mn_{0.1})SO$ on a log scale. Inset is the plot of the crystal structure of LaCuSO.

the Arrhenius equation $R = R_0{}^*exp(E_g/(k_B{}^*T))$, we obtained the activation energy $E_g \sim 0.14$ eV which is much smaller than 3.1 eV of the parent semiconductor LaCuSO.

Magnetic properties of $(La_{1-x}Ba_x)(Cu_{1-y}Mn_y)SO$ ($0 \le x \le 0.1$, $0.05 \le y \le 0.1$). In Fig. 2, we show the results of DC magnetic properties of $(La_{1-x}Ba_x)(Cu_{1-y}Mn_y)SO$ ($0 \le x \le 0.1, 0.05 \le y \le 0.1$). We plot the temperature dependence of the magnetization under field cooling (FC) and zero field cooling (ZFC) conditions with an applied external field of 100 Oe in Fig. 2a. In the measured temperature range, no anomaly or transition can be observed in $La(Cu_{0.9}Mn_{0.1})SO$, demonstrating that doping magnetic Mn atoms alone into LaCuSO can not result in any type of magnetic ordering. However, as marked by the red arrow for $x = 0.1$ and $y = 0.1$ sample, there is a sharp increase of the DC magnetization M in the temperature range of 140–150 K when both carriers and local magnetic moments are provided. The sudden sharp increase of DC magnetization is indicative of a ferromagnetic transition, which is denoted as the Curie temperature (T_C). T_C is $\sim$ 142 K for the doping levels of $x = 0.1$ and $y = 0.1$. In this case, (La,Ba) substitutions introduce the holes while (Cu,Mn) substitutions introduce the local magnetic moments, respectively. Hence, spins can be mediated by carriers, which will lead to the long range ferromagnetic ordering. It is consistent with Zener's model which is considered to explain the origin of ferromagnetism in (Ga,Mn)As system[6]. In Zener's model, the holes can mediate local moments arising from Mn spins through RKKY-like interaction effectively. Furthermore, we can also see the bifurcation between

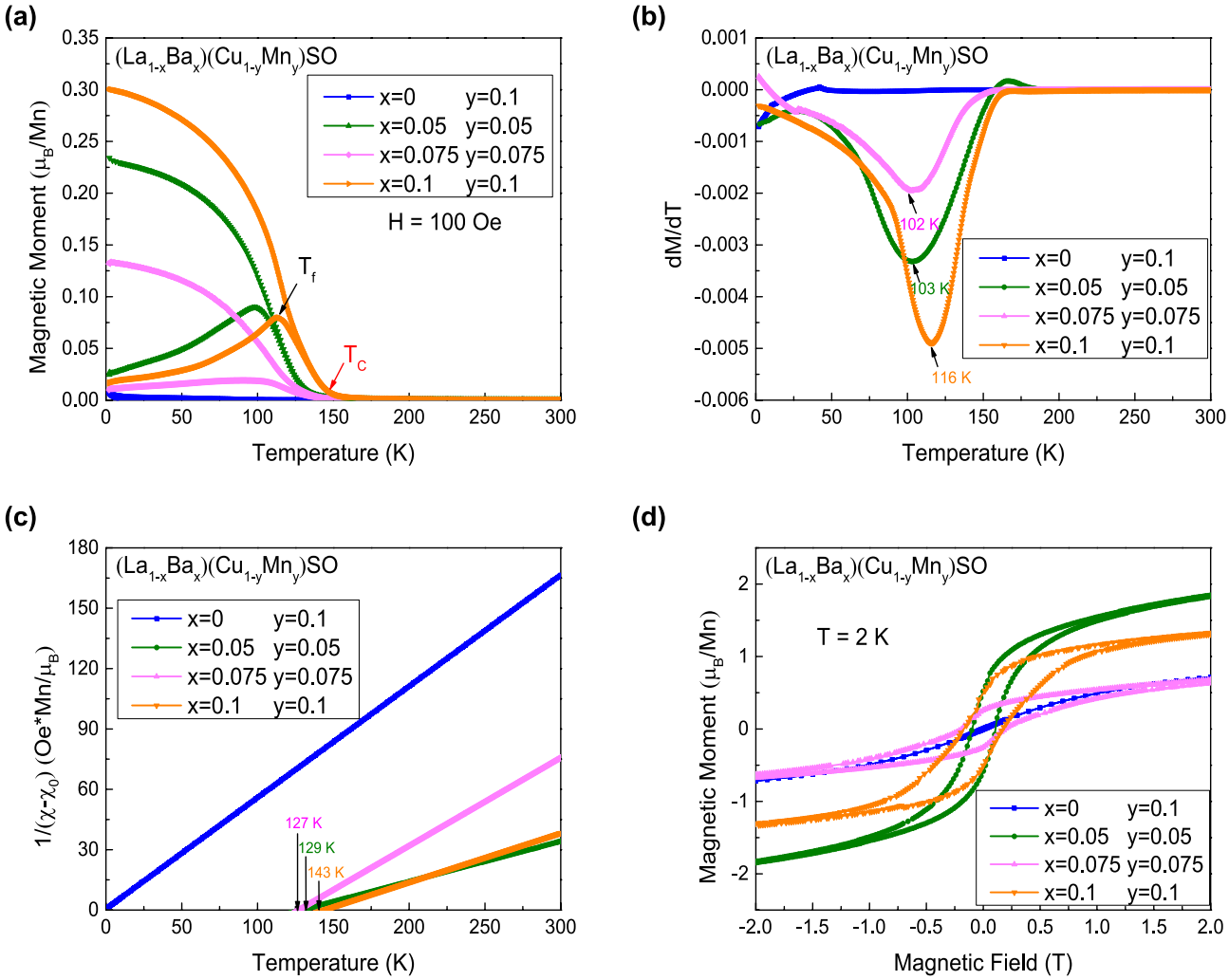

Figure 2. (**a**) Temperature dependent magnetization for $(La_{1-x}Ba_x)(Cu_{1-y}Mn_y)SO$ ($0 \le x \le 0.1$, $0.05 \le y \le 0.1$) measured in zero field cooling (ZFC) and field cooling (FC) condition under 100 Oe external field. The red arrow marks the Curie temperature (T_C) and the black arrow marks the freezing temperature (T_f) for $(La_{0.9}Ba_{0.1})(Cu_{0.9}Mn_{0.1})SO$, respectively. (**b**) The dM/dT versus T curves for $(La_{1-x}Ba_x)(Cu_{1-y}Mn_y)SO$ ($0 \le x \le 0.1, 0.05 \le y \le 0.1$). The arrows mark the temperature $T(dM/dT)$ for samples. (**c**) The reverse of $\chi - \chi_0$ versus temperature for $(La_{1-x}Ba_x)(Cu_{1-y}Mn_y)SO$ ($0 \le x \le 0.1, 0.05 \le y \le 0.1$). The arrows mark the Weiss temperature (θ) for samples. (**d**) The iso-thermal magnetic hysteresis measurement for $(La_{1-x}Ba_x)(Cu_{1-y}Mn_y)SO$ ($0 \le x \le 0.1, 0.05 \le y \le 0.1$) under 2 K.

FC and ZFC curves around 110 K. The temperature of the bifurcation is denoted as T_f, which is marked by the black arrow as shown in Fig. 2a, indicating the freezing temperature of individual spins or domain wall motion.

We plot the first derivative of magnetization versus temperature in Fig. 2b. Here, we focus on the temperature of the extreme point of dM/dT, which is denoted as $T(dM/dT)$. We find that the change of $T(dM/dT)$ with dopings is consistent with that of T_C. Theoretically, to accurately determine the Curie temperature T_C in a ferromagnetic compound, the method of Arrot plot can be used to define T_C explicitly[36]. That is, the iso-thermal magnetization data points (M^2 versus H/M) around T_C in high magnetic field would fall on a series of parallel lines. The line corresponding T_C would pass through the origin. Practically, we found this method would also bring some uncertainties. Instead, we found that $T(dM/dT)$ is proportional to T_C, and using $T(dM/dT)$ is very efficient and accurate to compare the variation of T_C for different samples. We also plot the inverse of DC susceptibility versus temperature in Fig. 2c. We can see that the curve of La($Cu_{0.9}Mn_{0.1}$)SO passes through the origin, which indicates that there is no magnetic transition. According to the Curie-Weiss law $\chi = \chi_0 + C/(T\text{-}\theta)$, the x-axis intercept of the linear fitting curves is defined as the Weiss temperature θ, where χ_0 is the temperature-independent component and C is the Curie constant. θ values are marked by vertical arrows in Fig. 2c, the variation trend of θ is consistent with that of T_C as well. Moreover, the positive θ values also indicate the ferromagnetic interaction between Mn-ions. Additionally, we found our "T_C" values are larger than $T(dM/dT)$, but smaller than the Weiss temperature θ (which is strictly determined by the intercept of $1/\chi$ versus T). We can also obtain the effective magnetic moment μ_{eff} from the formula $C = N\mu_0\mu_{eff}^2/3K_B$. The resultant μ_{eff} are in the order of magnitudes $\sim 5\ \mu_B/Mn$, which are much larger than those of spin glass ($\sim 0.01\ \mu_B/Mn$) but close to $5.9\ \mu_B/Mn$, as expected for fully magnetic individual Mn^{2+} moments[37,38]. In Fig. 2d, we plot the iso-thermal magnetization measured at 2 K. Similarly, ferromagnetic hysteresis loops can be observed for all polycrystals except La($Cu_{0.9}Mn_{0.1}$)SO. The obtained data for the Curie temperature T_C, the temperature $T(dM/dT)$, the Weiss temperature θ, the effective moment μ_{eff}, and the coercive field H_c are tabulated in Table 1.

Magnetic properties of ($La_{1-x}Ba_x$)($Cu_{0.95}Mn_{0.05}$)SO ($0 \le x \le 0.1$). Next, we investigate the influence of carriers on the ferromagnetic ordering by fixing the Mn concentration at $y = 0.05$. In Fig. 3, we display the results of DC magnetic properties of ($La_{1-x}Ba_x$)($Cu_{0.95}Mn_{0.05}$)SO ($0 \le x \le 0.1$). The temperature dependence of the magnetization under FC and ZFC conditions in an applied magnetic field of 100 Oe is shown in Fig. 3a. We can find a significant increase of M in the temperature range of 120–180 K for all curves. Interestingly, the more carrier doping levels, the higher T_C. T_C reaches to the maximum value of $\sim$ 170 K with Ba doping up to 10%.

Similarly, the first derivative of magnetization versus temperature and the inverse of DC susceptibility versus temperature are plotted in Fig. 3b and c, respectively. The variation trend of $T(dM/dT)$ and θ are the same as that of the T_C. It's worth noting that the effective moments are determined to be 3–5 μ_B/Mn under this circumstance, indicating that Mn-ion is in the high spin state $S = \frac{5}{2}$ with the valence of +2. μ_{eff} are all less than the expected value of $5.9\ \mu_B/Mn$, which are similar to the situation in (Ga,Mn)As system[39,40]. In general, the effective moments are affected by the valence of Mn ions, and the indirect interaction arising from carriers mediated ferromagnetism and the direct antiferromagnetic interaction of Mn atoms at nearest-neighbor sites. When we calculate the effective moments, we suppose all doped Mn atoms are involved into the magnetic interaction. While small amount of diluted Mn atoms may not effectively interact with carriers but they were counted in. This may be another reason that the effective magnetic moments are much smaller than the $5.9\ \mu_B/Mn$ expected for $S = \frac{5}{2}$. We also display the iso-thermal magnetization at 2 K in Fig. 3d. All specimens show clear hysteresis loops, suggesting that the ferromagnetic transition has fully developed. However, the variations of coercive field and saturation moment in Figs. 2d and 3d are not monotonous with the increasing doping, which might be due to the result of competition between ferromagnetic coupling via the RKKY-like interaction and the nearest-neighbor antiferromagnetic coupling via direct exchange interaction. Likewise, the obtained data for the Curie temperature T_C, the temperature $T(dM/dT)$, the Weiss temperature θ, the effective moment μ_{eff}, and the coercive field H_c are tabulated in Table 1.

Discussion and summary

We have successfully synthesized a new bulk form Cu-based MS (La,Ba)(Cu,Mn)SO by solid-state reaction method, which is iso-structural to the iron-based 1111-type superconductor LaFeAsO. The maximum T_C can reach up to $\sim$ 170 K when the doping levels of Ba and Mn are 10% and 5%, respectively. These results demonstrate that the ferromagnetic transition occurs only when both carriers and spins are introduced. However, the competition between ferromagnetic coupling and antiferromagnetic coupling may have a considerable influence on the ferromagnetism. Additionally, the Weiss temperature θ is defined as the "Curie temperature T_C" in (La,Sr)(Cu,Mn)SO[32]. We now compare the Weiss temperature θ for the same doping levels of (La,Sr)(Cu,Mn)SO and (La,Ba)(Cu,Mn)SO. The θ of ($La_{0.925}Sr_{0.075}$)($Cu_{0.925}Mn_{0.075}$)SO is $\sim$ 200 K. However, the θ of ($La_{0.925}Ba_{0.075}$)($Cu_{0.925}Mn_{0.075}$)SO decreases by $\sim$ 37% to 127 K. This is apparently because the ionic radius of Ba^{2+} (1.36 Å) is larger than that of Sr^{2+} (1.18 Å), as can be seen that (La,Ba)(Cu,Mn)SO has larger bond length than that of (La,Sr)(Cu,Mn)SO. Consequently, the ferromagnetic interaction in (La,Ba)(Cu,Mn)SO is suppressed. This phenomenon has also been observed in $Ba(Zn,Co)_2As_2$[30] and (La,Ca)(Zn,Mn)AsO[31]. To summarize, this new bulk MS can be used as a new reference to study the origin of ferromagnetism in magnetic semiconductors with higher T_C.

Methods

Material synthesis. We synthesized ($La_{1-x}Ba_x$)($Cu_{1-y}Mn_y$)SO ($0 \le x \le 0.1$, $0 \le y \le 0.1$) polycrystalline specimens by solid-state reaction with high-purity starting materials of La, La_2O_3, MnS, CuS and BaO_2. According to the chemical formula, we mixed and slowly heated the ingredients up to 950 °C in an evacuated silica tube,

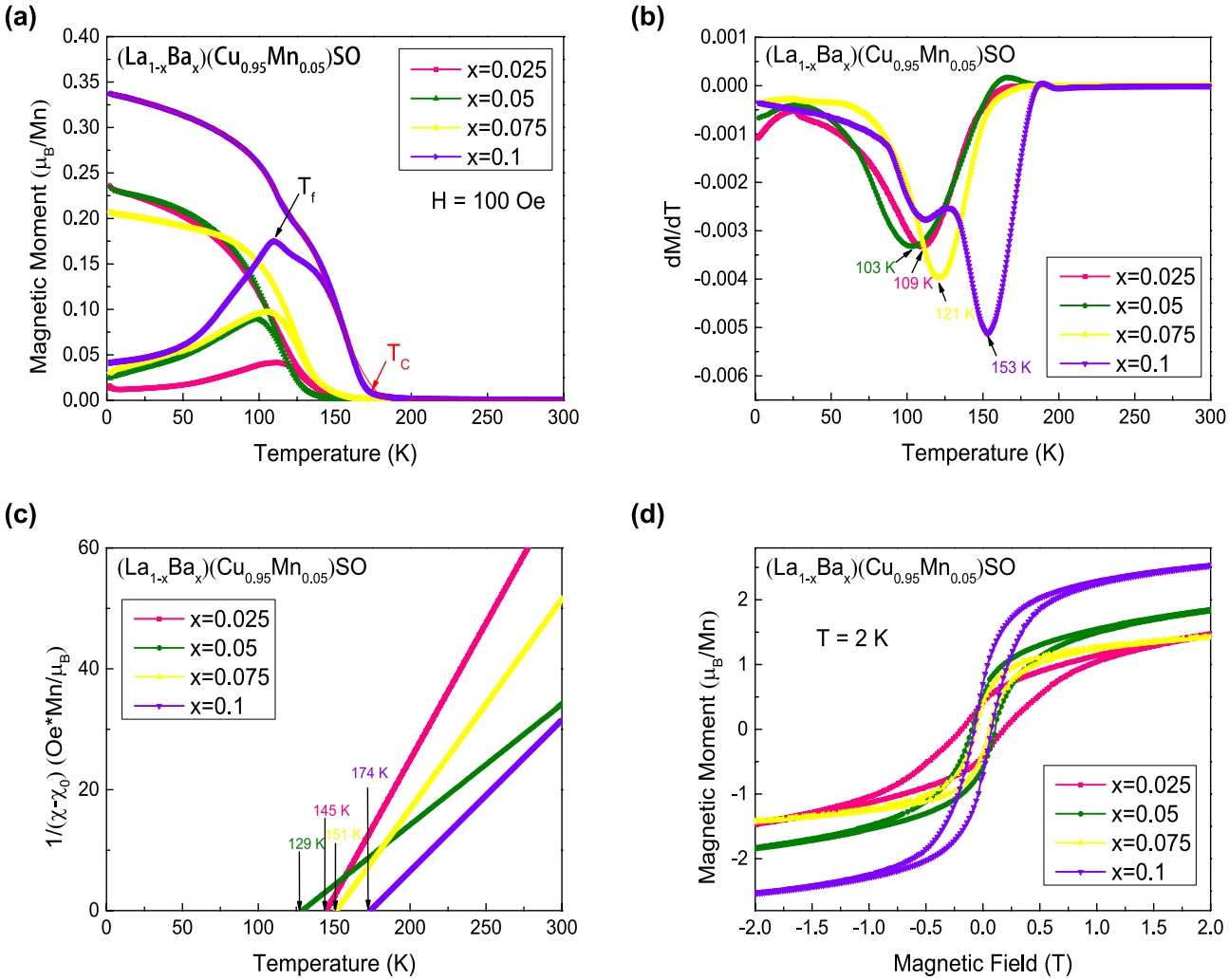

Figure 3. (**a**) Temperature dependent magnetization for $(La_{1-x}Ba_x)(Cu_{0.95}Mn_{0.05})SO$ $(0 \leq x \leq 0.1)$ measured in zero field cooling (ZFC) and field cooling (FC) condition under 100 Oe external field. The red arrow marks the Curie temperature (T_C) and the black arrow marks the freezing temperature (T_f) for $x = 0.1$, respectively. (**b**) The dM/dT versus T curves for $(La_{1-x}Ba_x)(Cu_{0.95}Mn_{0.05})SO$ $(0 \leq x \leq 0.1)$. The arrows mark the temperature $T(dM/dT)$ for samples. (**c**) The reverse of $\chi - \chi_0$ versus temperature for $(La_{1-x}Ba_x)(Cu_{0.95}Mn_{0.05})SO$ $(0 \leq x \leq 0.1)$. The arrows mark the Weiss temperature (θ) for samples. (**d**) The iso-thermal magnetic hysteresis measurement for $(La_{1-x}Ba_x)(Cu_{0.95}Mn_{0.05})SO$ $(0 \leq x \leq 0.1)$ under 2 K.

$x; y$	T_C (K)	$T(dM/dT)$ (K)	θ (K)	μ_{eff} (μ_B/Mn)	H_c (Oe)
0; 0.1	–	–	–	2.5	–
0.075; 0.075	121	102	127	3.2	1910
0.1; 0.1	142	116	143	4.3	1807
0.025; 0.05	131	109	145	3.1	1808
0.05; 0.05	126	103	129	4.7	1005
0.075; 0.05	140	121	151	3.6	598
0.01; 0.05	170	153	174	4.2	805

Table 1. The Curie temperature T_C, the temperature $T(dM/dT)$, the Weiss temperature θ, the effective moment μ_{eff} and the coercive field H_c for $(La_{1-x}Ba_x)(Cu_{1-y}Mn_y)SO$ $(0 \leq x \leq 0.1, 0.05 \leq y \leq 0.1)$.

where the mixture was held for about 33 h before cooling down to the room temperature. Secondly, the products were grounded, pelleted, and sintered at 950 °C for another 33 h again to achieve complete reaction.

Experimental characterization. Powder x-ray diffraction was performed at room temperature using a PANalytical x-ray diffractometer (model EMPYREAN) with monochromatic Cu $K_{\alpha 1}$ radiation. The DC magnetic properties of the polycrystals were conducted by using a Quantum Design magnetic property measurement system (MPMS-3). The electrical resistivity was measured on sintered pellets by a Quantum Design physical property measurement system (PPMS).

Data availability

All data generated or analysed during this study are included in this published article or available from the corresponding author on reasonable request.

Received: 14 June 2023; Accepted: 1 September 2023
Published online: 05 September 2023

References

1. Munekata, H. *et al.* Diluted magnetic III-V semiconductors. *Phys. Rev. Lett.* **63**, 1849 (1989).
2. Ohno, H. *et al.* (Ga, Mn)As: A new diluted magnetic semiconductor based on GaAs. *Appl. Phys. Lett.* **69**, 363–365 (1996).
3. Jungwirth, T., Sinova, J., Mašek, J., Kučera, J. & MacDonald, A. Theory of ferromagnetic (III, Mn)V semiconductors. *Rev. Mod. Phys.* **78**, 809 (2006).
4. Nam Hai, P. *et al.* Growth and characterization of n-type electron-induced ferromagnetic semiconductor (In, Fe)As. *Appl. Phys. Lett.* **101**, 182403 (2012).
5. Tu, N. T., Hai, P. N., Anh, L. D. & Tanaka, M. High-temperature ferromagnetism in heavily Fe-doped ferromagnetic semiconductor (Ga, Fe)Sb. *Appl. Phys. Lett.* **108**, 192401 (2016).
6. Dietl, T., Ohno, O. H., Matsukura, A. F., Cibert, J. & Ferrand, E. D. Zener model description of ferromagnetism in zinc-blende magnetic semiconductors. *Science* **287**, 1019–1022 (2000).
7. Wang, M. *et al.* Achieving high curie temperature in (Ga, Mn)As. *Appl. Phys. Lett.* **93**, 132103 (2008).
8. Chiba, D., Takamura, K., Matsukura, F. & Ohno, H. Effect of low-temperature annealing on (Ga, Mn)As trilayer structures. *Appl. Phys. Lett.* **82**, 3020–3022 (2003).
9. Chen, L. *et al.* Low-temperature magnetotransport behaviors of heavily Mn-doped (Ga, Mn)As films with high ferromagnetic transition temperature. *Appl. Phys. Lett.* **95**, 182505 (2009).
10. Chen, L. *et al.* Enhancing the Curie temperature of ferromagnetic semiconductor (Ga, Mn)As to 200 K via nanostructure engineering. *Nano Lett.* **11**, 2584–2589 (2011).
11. Pulizzi, F. Is it really intrinsic ferromagnetism?. *Nat. Mater.* **9**, 956–957 (2010).
12. Potashnik, S. *et al.* Effects of annealing time on defect-controlled ferromagnetism in $Ga_{1-x}Mn_xAs$. *Appl. Phys. Lett.* **79**, 1495–1497 (2001).
13. Yanagi, H. *et al.* Magnetic and carrier transport properties of Mn-doped p-type semiconductor LaCuOSe: An investigation of the origin of ferromagnetism. *J. Appl. Phys.* **100**, 033717 (2006).
14. Deng, Z. *et al.* Li(Zn, Mn)As as a new generation ferromagnet based on a I-II-V semiconductor. *Nat. Commun.* **2**, 422 (2011).
15. Deng, Z. *et al.* Diluted ferromagnetic semiconductor Li(Zn, Mn)P with decoupled charge and spin doping. *Phys. Rev. B* **88**, 081203 (2013).
16. Wang, Q. *et al.* $Li_{1.1}(Zn_{1-x}Cr_x)As$: Cr doped I-II-V diluted magnetic semiconductors in bulk form. *J. Appl. Phys.* **115**, 083917 (2014).
17. Zhao, K. *et al.* Ferromagnetism at 230 K in $(Ba_{0.7}K_{0.3})(Zn_{0.85}Mn_{0.15})_2As_2$ diluted magnetic semiconductor. *Chin. Sci. Bull.* **59**, 2524–2527 (2014).
18. Zhao, K. *et al.* New diluted ferromagnetic semiconductor with Curie temperature up to 180 K and isostructural to the '122' iron-based superconductors. *Nat. Commun.* **4**, 1442 (2013).
19. Guo, S. *et al.* $Ba(Zn, Co)_2As_2$: A diluted ferromagnetic semiconductor with n-type carriers and isostructural to 122 iron-based superconductors. *Phys. Rev. B* **99**, 155201 (2019).
20. Ding, C. *et al.* $(La_{1-x}Ba_x)(Zn_{1-x}Mn_x)AsO$: A two-dimensional 1111-type diluted magnetic semiconductor in bulk form. *Phys. Rev. B* **88**, 041102 (2013).
21. Wang, X. *et al.* The superconductivity at 18 K in LiFeAs system. *Solid State Commun.* **148**, 538–540 (2008).
22. Rotter, M., Tegel, M. & Johrendt, D. Superconductivity at 38 K in the iron arsenide $(Ba_{1-x}K_x)Fe_2As_2$. *Phys. Rev. Lett.* **101**, 107006 (2008).
23. Kamihara, Y., Watanabe, T., Hirano, M. & Hosono, H. Iron-based layered superconductor $La[O_{1-x}F_x]FeAs$ (x=0.05-0.12) with T_C =26K. *J. Am. Chem. Soc.* **130**, 3296–3297 (2008).
24. Dunsiger, S. *et al.* Spatially homogeneous ferromagnetism of (Ga, Mn)As. *Nat. Mater.* **9**, 299–303 (2010).
25. Ding, C., Qin, C., Man, H., Imai, T. & Ning, F. NMR investigation of the diluted magnetic semiconductor $Li(Zn_{1-x}Mn_x)P$ (x=0.1). *Phys. Rev. B* **88**, 041108 (2013).
26. Guo, S. & Ning, F. Progress of novel diluted ferromagnetic semiconductors with decoupled spin and charge doping: Counterparts of Fe-based superconductors. *Chin. Phys. B* **27**, 097502 (2018).
27. Gu, Y., Guo, S. & Ning, F. Progress on microscopic properties of diluted magnetic semiconductors by NMR and μSR. *J. Semicond.* **40**, 081506 (2019).
28. Peng, Y. *et al.* Effects of chemical pressure on diluted magnetic semiconductor $(Ba, K)(Zn, Mn)_2As_2$. *Chin. Phys. B* **28**, 057501 (2019).
29. Sun, F. *et al.* Pressure effect on the magnetism of the diluted magnetic semiconductor $(Ba_{1-x}K_x)(Zn_{1-y}Mn_y)_2As_2$ with independent spin and charge doping. *Phys. Rev. B* **93**, 224403 (2016).
30. Fu, L. *et al.* Drastic improvement of Curie temperature by chemical pressure in N-type diluted magnetic semiconductor $Ba(Zn, Co)_2As_2$. *Sci. Rep.* **11**, 7652 (2021).
31. Zhang, R. *et al.* Manipulation of the ferromagnetic ordering in magnetic semiconductor (La, Ca)(Zn, Mn)AsO by chemical pressure. *J. Magn. Magn. Mater.* **554**, 169276 (2022).
32. Yang, X. *et al.* Sr and Mn co-doped LaCuSO: A wide band gap oxide diluted magnetic semiconductor with T_C around 200 K. *Appl. Phys. Lett.* **103**, 022410 (2013).
33. Ueda, K., Inoue, S., Hosono, H., Sarukura, N. & Hirano, M. Room-temperature excitons in wide-gap layered-oxysulfide semiconductor: LaCuOS. *Appl. Phys. Lett.* **78**, 2333–2335 (2001).

34. Ueda, K., Inoue, S., Hirose, S., Kawazoe, H. & Hosono, H. Transparent p-type semiconductor: LaCuOS layered oxysulfide. *Appl. Phys. Lett.* **77**, 2701–2703 (2000).
35. Toby, B. H. & Von Dreele, R. B. GSAS-II: The genesis of a modern open-source all purpose crystallography software package. *J. Appl. Crystallogr.* **46**, 544–549 (2013).
36. Arrott, A. Criterion for ferromagnetism from observations of magnetic isotherms. *Phys. Rev.* **108**, 1394 (1957).
37. Tholence, J. & Tournier, R. Susceptibility and remanent magnetization of a spin glass. *Le Journal de Physique Colloques* **35**, C4-229 (1974).
38. Monod, P., Prejean, J. & Tissier, B. Magnetic hysteresis of CuMn in the spin glass state. *J. Appl. Phys.* **50**, 7324–7329 (1979).
39. Jungwirth, T. *et al.* Low-temperature magnetization of (Ga, Mn)As semiconductors. *Phys. Rev. B* **73**, 165205 (2006).
40. Wang, K. *et al.* Influence of the Mn interstitial on the magnetic and transport properties of (Ga, Mn)As. *J. Appl. Phys.* **95**, 6512–6514 (2004).

Acknowledgements

The work at Zhejiang was supported by National Key R &D Program of China (No. 2022YFA1402701, 2022YFA1403202), NSF of China (No. 12074333), the Key R &D Program of Zhejiang Province, China (2021C01002).

Author contributions

F.L.N., J.O.D. and C.D. conceived this work, J.O.D. conducted the experiments with the help of C.D., X.Q.Z., L.F.X. and X.P., results were analysed by J.O.D., Q.L.Y., L.C.F., Y.L.G. and G.X.Z., all authors contributed to the preparation of this manuscript.

Competing interests

The authors declare no competing interests.

Additional information

Correspondence and requests for materials should be addressed to F.N.

Reprints and permissions information is available at www.nature.com/reprints.

Publisher's note Springer Nature remains neutral with regard to jurisdictional claims in published maps and institutional affiliations.